Heat Transfer Characteristics Evaluation of Multi-Elbow Cooling System for Fusion Divertor under One-Sided Heating*)

Shinji EBARA, Kenya MITOBE, Yukinori HAMAJI[1] and Hidetoshi HASHIZUME

Tohoku University, 6-6-01-2 Aramaki-Aza-Aoba, Aoba-ku, Sendai, Miyagi 980-8579, Japan

[1]*National Institute for Fusion Science, 322-6 Oroshi-cho, Toki, Gifu 509-5292, Japan*

(Received 9 January 2023 / Accepted 13 March 2023)

In this study, a cooling system for fusion reactor divertor that utilizes a swirling flow generated downstream of multi-elbow piping was proposed, and flow fields of the multi-elbow piping (triple elbow) were investigated using flow visualization experiment. Additionally, heat transfer experiment was conducted under one-sided heating condition to simulate a fusion reactor environment. The results revealed that the heat flux removed by the swirling flow in the elbow piping exceeded the critical heat flux in straight piping, and a heat removal performance of up to 25 MW/m^2 was achieved.

Keywords: divertor cooling, boiling heat transfer, multi-elbow piping, swirling flow, one-sided heating

DOI: 10.1585/pfr.18.2405034

1. Introduction

Cooling the fusion divertor is a major challenge in fusion reactor development. Extremely high heat flux of more than 10 MW/m^2 is assumed to be imposed on the International Thermonuclear Experimental Reactor (ITER) divertor [1] in which swirl tubes with twisted tapes are used as a heat transfer and critical heat flux (CHF) promoter. The swirling flow generated within the swirl tube promotes heat transfer and CHF enhancement; however, the use of swirl tubes presents some engineering challenges, such as difficulties in fabrication and increased pressure loss due to the twisted tape insertion.

Kodate *et al.* proposed a cooling system that uses a swirling flow generated downstream of three-dimensionally connected multi-elbow piping as a potential alternative to the swirl tube [2]. This system is expected to address the engineering issues associated with the swirl tube, owing to its simpler structure and smaller pressure loss. In previous studies, visualization experiments were conducted to optimize the geometrical parameters of elbow pipings [2]. The results revealed that the strongest swirling flow was generated in the triple elbow piping configuration when elbows with a small radius of curvature ratio and 3D+3D layout were used [3]. Additionally, a heat transfer experiment with ohmic heating was conducted to evaluate the heat transfer performance for both single-phase flow and whole circumferential heating conditions [4]. The results revealed that the heat transfer efficiency ≤80% compared to a swirl tube with a twisted ratio of 2.0 [4]. However, the heat transfer performance for two-phase flow under one-sided heating condition similar to real fusion reactor was not evaluated [4].

This study aims to assess the suitability of divertor cooling system under one-sided heating condition using the swirling flow generated downstream of a three-dimensionally connected triple elbow as an alternative to the swirl tube. A flow visualization experiment was conducted to evaluate the time-averaged flow field of the swirling flow in an 18 mm inner diameter triple elbow piping, followed by a heat transfer experiment to assess the subcooled boiling heat transfer characteristics under one-sided heating condition.

2. Experimental Setups

2.1 Flow visualization experiment

Figure 1 shows the experimental apparatus employed in this study. Two-dimensional particle image velocimetry (PIV) was used to evaluate the secondary flow in cross-

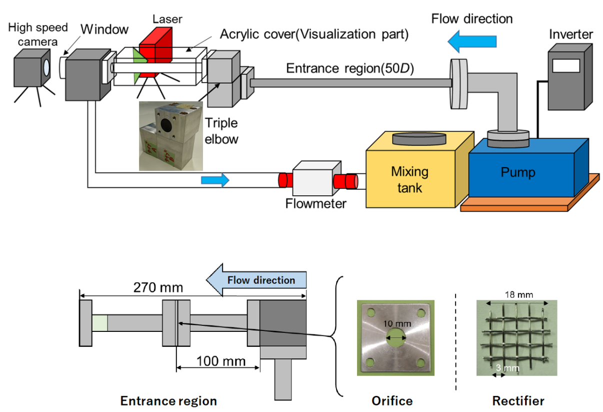

Fig. 1 Apparatus of the visualization experiment.

author's e-mail: shinji.ebara.e6@tohoku.ac.jp

*) This article is based on the presentation at the 31st International Toki Conference on Plasma and Fusion Research (ITC31).

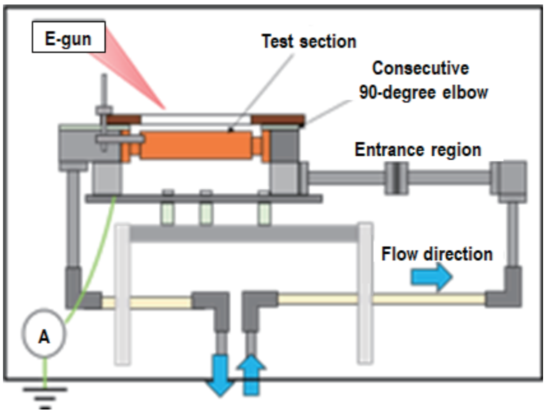

Fig. 2 Apparatus of the heat transfer experiment.

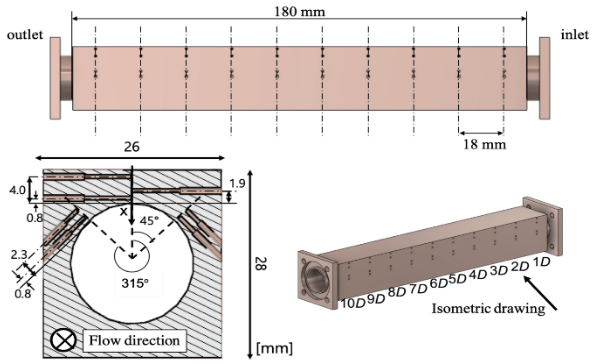

Fig. 3 Schematic of the test section for heat transfer experiment and TC locations.

sections perpendicular to the pipe axis. A diode laser with wavelength of 808 nm and maximum power of 200 W (maximum pulse energy of 15 mJ) was used. The high-speed camera used had a resolution of 1024×1024 pixels and was capable of capturing 2,048 images per shot at a frame rate of 60 and VidPIV was used as the analysis software. Tap water was used as the working fluid, with a nylon particle tracer of 20 µm diameter. In the heat transfer experiment using ACT2, as described later, a fully developed pipe turbulent flow entrance was not installed due to spatial limitations. In order to achieve an axisymmetric flow similar to the developed flow as the inflow at the elbow inlet, an orifice and a wire mesh sheet were installed upstream of the elbow inlet as shown in Fig. 2. The same flow channel structure was used in the flow visualization experiment to evaluate the flow field in the heat transfer experiment. The Reynolds number (*Re*), inlet temperature (T_{in}), and the pipe inner diameter (D) were set to 2.0×10^4, 315 K, and 18 mm, respectively. Triple elbow comprised three 90-degree elbows with the same curvature ratio of 1.0. Visualization measurements were taken at $1.5D$ downstream of the third elbow outlet, $9.5D$, and from $2D$ to $9D$ at $1D$ interval for the pipe cross-section.

2.2 Heat transfer experiment

Figure 2 shows the apparatus used in the heat transfer experiment. The heat load was applied using a super high heat flux test device ACT2 (Active Cooling Teststand) [5] at the National Institute for Fusion Science. The device employs a large-scale electron beam to impose a uniform heat flux on an irradiated surface in a vacuum chamber. The experimental apparatus comprised a closed loop with a tank, flowmeter with pressure gage outside the chamber, an elbow section, and a heat transfer test section inside the vacuum chamber. All sections in the chamber were circular channels with an inner diameter of 18 mm. The experiment was conducted under steady-state condition for about 100 s.

Figure 3 shows the copper test section used in the experiments with the minimum distance of 5 mm between the irradiated surface and cooling surface. To estimate the tube wall temperature and the heat flux flowing into the tube on the x-axis in Fig. 3, the temperature distribution in the x-axis was linearly extrapolated to the cooling surface using two measured temperatures closer to it. The temperature of the heated surface was monitored by the thermocouples closest to it to prevent the surface from melting. The boiling curves were obtained from the estimated tube wall temperature and inflow heat flux and then compared with the following empirical equations. In nonboiling situations, the heat transfer via single-phase flow was compared with the Dittus-Boelter correlation equation presented in Equation (1).

$$Nu = 0.023 Re^{0.8} Pr^{0.4}. \tag{1}$$

In the case of partial nucleate boiling, the heat transfer by two-phase forced convection was compared using Rohsenow's equation [6], as shown in Equation (2), which is equal to the heat transfer by single-phase forced convection plus the heat transfer by pool boiling, as shown in Equation (3) [7].

$$\frac{c_{pl}(T_{\mathrm{w}} - T_{\mathrm{sat}})}{H_{lg}} = C_{sf} \left[\frac{q_{\mathrm{BO}}}{\mu_{\mathrm{l}} H_{\mathrm{lg}}} \sqrt{\frac{\sigma}{g(\rho_{\mathrm{l}} - \rho_{\mathrm{g}})}} \right]^{0.33} \mathrm{Pr}^{1.7}, \tag{2}$$

$$q_{\mathrm{W}} = q_{\mathrm{CON}} + q_{\mathrm{BO}}. \tag{3}$$

Water was used as the working fluid with a pressure of 2 atm and saturation temperature of 493.9 K. The Reynolds number used were 1.2×10^4 and 2.4×10^4 for volumetric flow rates of 10 and 20 L/min, respectively. The fluid inlet temperature was set to 317 K.

3. Results and Discussion

3.1 Flow visualization experiment

Figure 4 shows the time-averaged velocity fields normalized by the mean axial velocity in the pipe cross-section range of $1.5D$ - $9.5D$ downstream of the outlet of triple elbows. These figures show that a swirling flow appears in the entire cross-section, and its velocity is higher near the pipe wall. The maximum circumferential velocity of the swirling flow is ≤50% of the mean axial flow velocity, and the intensity of the swirling flow decreases as it flows downstream.

3.2 Heat transfer experiment

The experimental temperature measurement results are presented as comparisons between the test sections downstream of the elbow outlet and straight piping for volumetric flow rates of 10 and 20 L/min, corresponding to Reynolds number of 1.2×10^4 and 2.4×10^4, respectively.

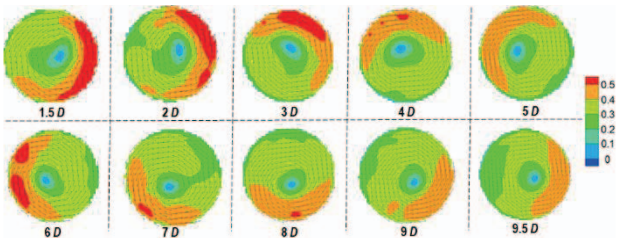

Fig. 4 Time-averaged velocity fields in the pipe cross-sections downstream of the triple elbow outlet.

Figure 5 illustrates the correlation between the measured temperatures closest to the cooling surface (0.8 mm from the cooling surface) and the incident heat flux obtained at 72 (4*D*) and 162 mm (9*D*) downstream of the elbow outlet in the straight piping case. The results of the flow visualization experiment indicate a counterclockwise swirling flows occurred toward the flow direction, which implies the position of 45° in Fig. 4 is located upstream of those of 0° and 315°. Furthermore, the temperature of the channel wall at 45° tends to decrease due to the swirling flow generated downstream of the triple elbow. For both cases, elbow piping and straight piping, small temperature change was observed for incident heat flux of ≤10 MW/m^2. However, for volumetric flow rate of 20 L/min with incident heat flux of > 10 MW/m^2, the temperature of the elbow case decreased to ≤70 K.

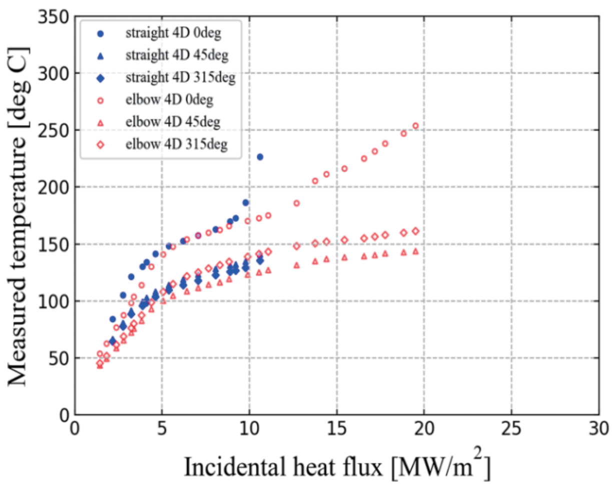

(a) 10 L/min, 4*D*

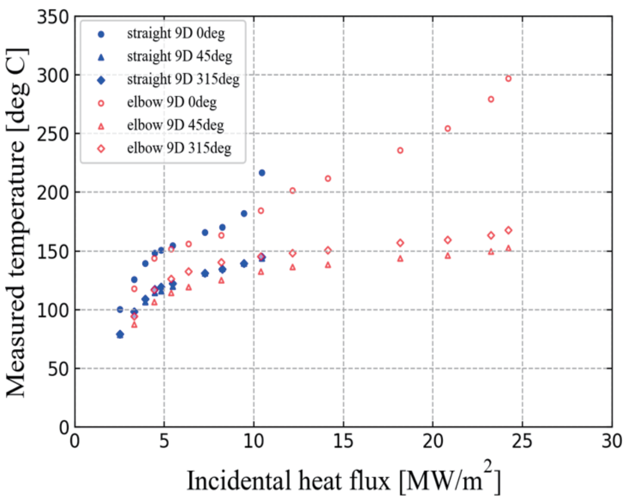

(b) 10 L/min, 9*D*

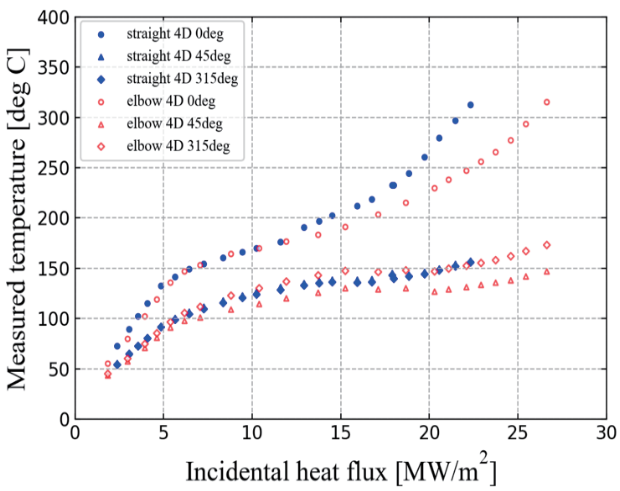

(c) 20 L/min, 4*D*

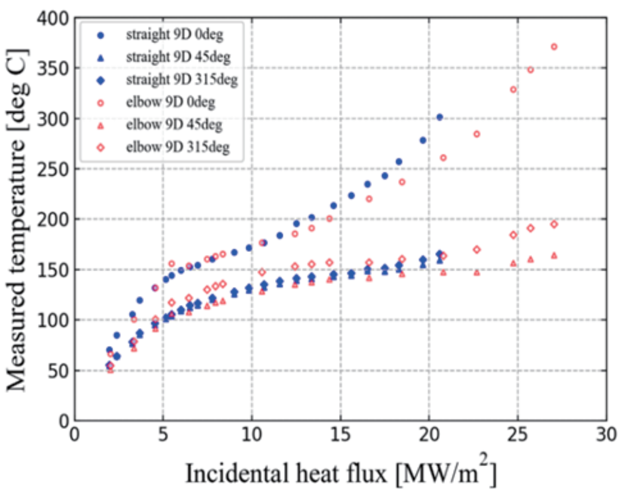

(d) 20 L/min, 9*D*

Fig. 5 Relationship between the measured temperature closest to the cooling surface (0.8 mm from the cooling surface) and the incident heat flux obtained 4*D* and 9*D* downstream of the elbow outlet compared to those obtained from the straight piping.

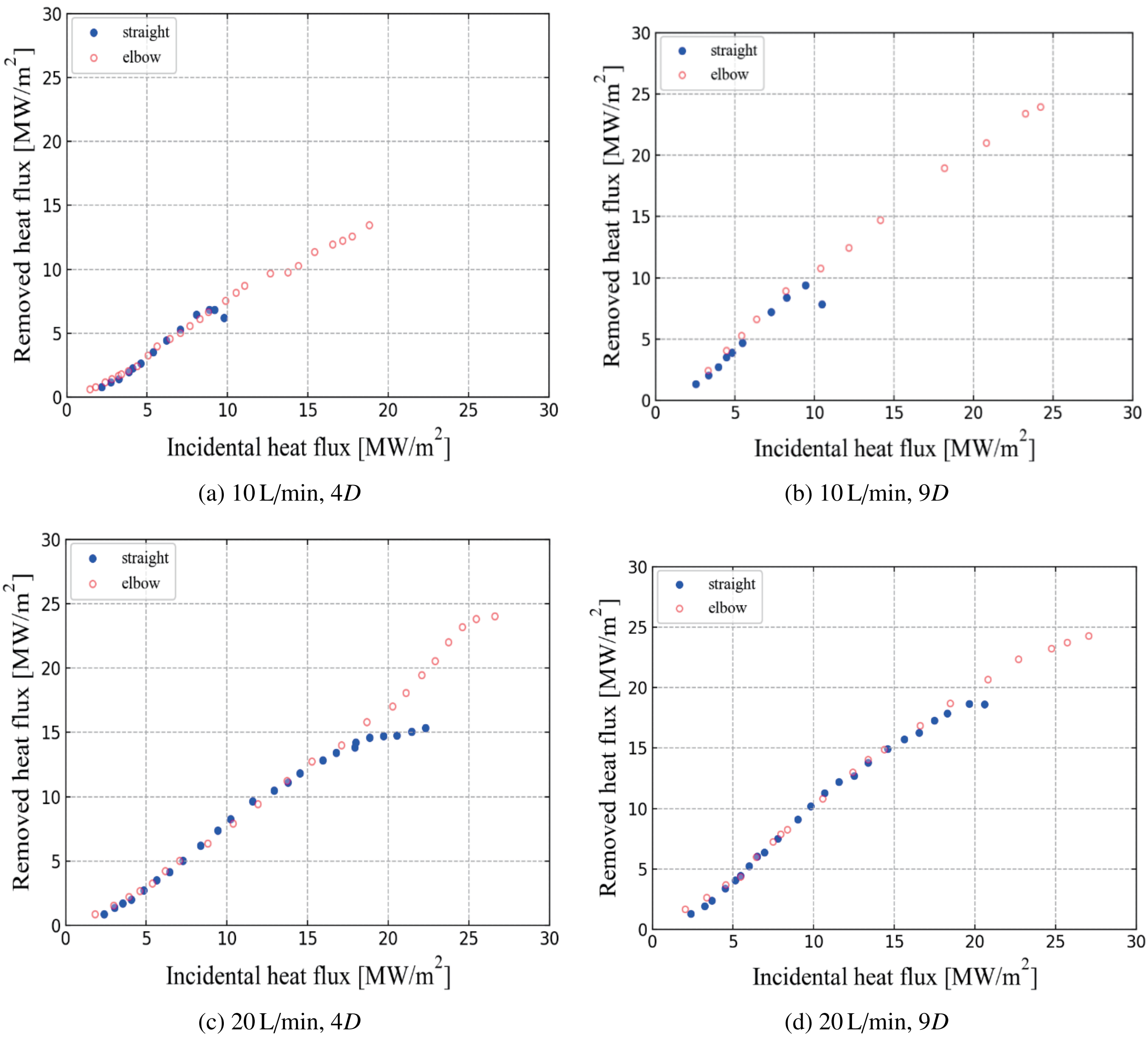

Fig. 6 Relationship between the removed heat flux and incident heat flux.

Contrarily, the measured temperatures in the downstream side of the swirling flow, which correspond to the data plotted as “315 deg” in Fig 5, were higher than those in the upstream side of the swirling flow plotted as “45 deg”. The temperature data showed good agreement with the flow direction of the swirling flow. The maximum temperature difference between the two cases was about 70 K at 4*D* downstream of the elbow outlet, while that about 40 K at 9*D* downstream. As described, the temperature difference between those obtained at 45° and 315° became small in the downstream region of the axial mean flow. This finding was consistent with the result from the visualization experiment, which showed that the swirling flow dampens in the downstream region.

Figure 6 shows the relationship between the removed heat flux and the incident heat flux measured at 4*D* and 9*D*, respectively, downstream of the elbow outlet. In the straight piping, the removed heat flux tends to reach a plateau of ~9 MW/m^2 for a volumetric flow rate of 10 L/min and ~19 MW/m^2 in the case of 20 L/min. In the case of the elbow piping, the removed heat flux increases monotonically with the incident heat flux imposed. This can be attributed to the enhanced cooling limit of the elbow piping. In the case of straight piping, doubling the volumetric flow rate roughly doubled the value of the removed heat flux reaching the plateau. However, in the case of elbow piping, no cooling limit was observed in the experiment, even when the volumetric flow rate was changed. The reason behind this phenomenon needs to be examined in the future.

Figure 7 depicts the maximum heat fluxes measured at each measurement position. Unfortunately, data are not available for some cases, including 10 L/min, straight 7*D*; 20 L/min, elbow 8*D*; 20 L/min, elbow 7*D*; and 20 L/min, elbow 8*D* due to measurement faults. Furthermore, the data obtained at 1*D* and 10*D*, which represent the ends of the test sections, are excluded from the analysis as they are assumed to have end effects. With a few exceptions

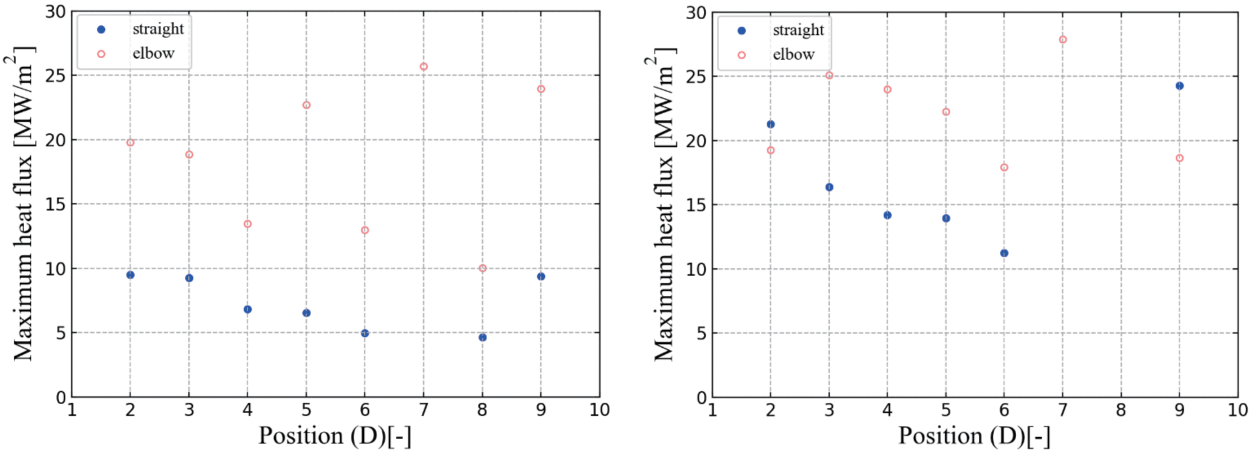

(a) 10 L/min (b) 20 L/min

Fig. 7 Relationship between the measured position and maximum heat flux.

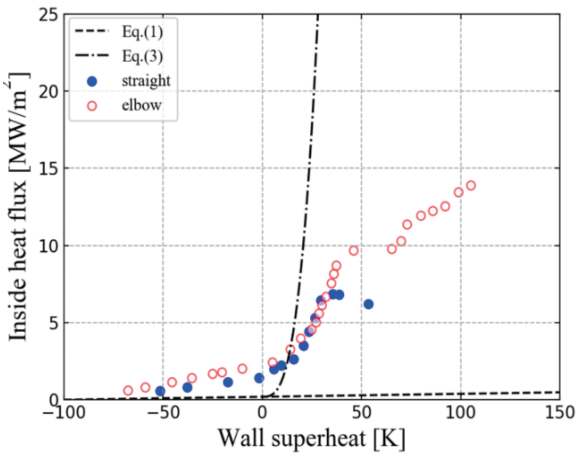

(a) 10 L/min, 4*D*

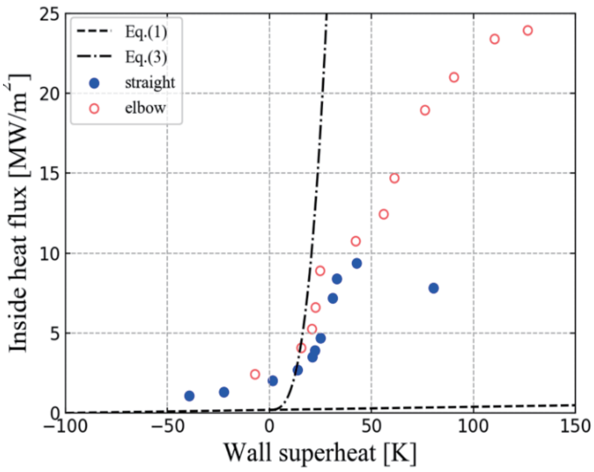

(b) 10 L/min, 9*D*

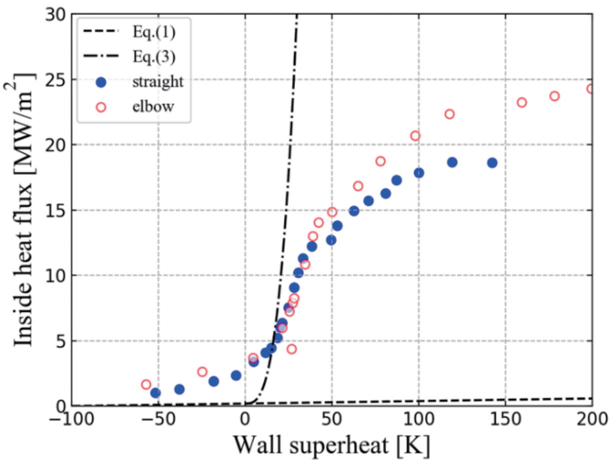

(c) 20 L/min, 4*D*

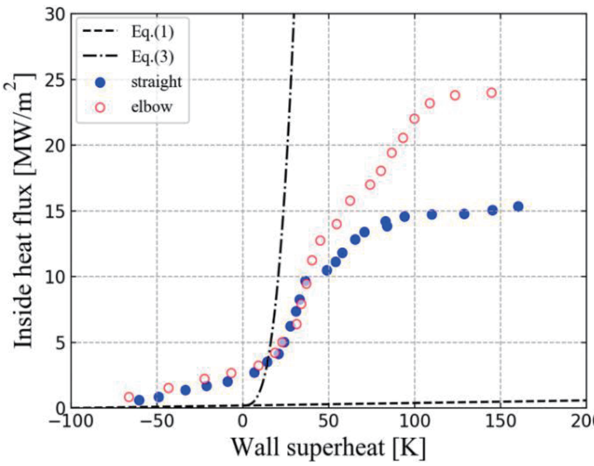

(d) 20 L/min, 9*D*

Fig. 8 Boiling curve obtained at 4*D* and 9*D* downstream.

(20 L/min, elbows 2*D* and 9*D*), the maximum heat flux in the elbow piping exceeds that of the straight piping. However, the tendency of the maximum heat flux in the elbow piping from upstream to downstream is not consistent and does not align with the swirling flow tendency observed in the visualization experiment (more downstream of the elbow outlet the piping flow flows, the less strong the swirl flow becomes). The results could be due to measurement

errors in the temperature used to calculate the removed heat flux or difference in the surface roughness of the cooling surface. Further experiments are necessary to investigate the cause.

Figure 8 shows the boiling curves obtained at $4D$ and $9D$ downstream of the elbow outlet. Each boiling curve is divided into nonboiling and nucleate boiling regions. The obtained boiling curves reveal that the onset of boiling appears at ~5 MW/m^2 regardless of the flow rate. In the nucleate boiling region, heat transfer via boiling is more dominant than that by convection; therefore, there was no significant difference between the elbow and straight piping. For comparison, Equation (3), which is the sum of the heat transfer effects of convection expressed using Dittus-Boelter's Equation (1) and boiling using Rohsenow's Equation (2), is plotted in Fig. 8. The experimental data do not agree with the equations in all regions, which can be due to the small heating region, measurement error, and evaluation method of the inside heat flux. Equation (1) was obtained in a thermally fully developed situation, while the experimental data were obtained in the condition where the heated region was considerably limited to $1D \times 1D$. Therefore, the heat flux of the nonboiling region in the experiment is higher than that in Equation (1). Moreover, the inside heat flux evaluated by assuming a linear temperature change near the cooling surface may not be correct, particularly in the case of high incident heat flux because of the increase in temperature gradient due to the heat flow contraction effect on the cooling surface. This effect is likely to be more pronounced in the boiling region.

Although CHF was not observed, it was found that the heat flux did not increase with increasing wall temperature, indicating the limit of partial cooling. In the straight piping with a volume flow rate of 10 L/min, the wall heat flux reached a plateau of ~6 MW/m^2 at $4D$ downstream of the elbow outlet and ~8 MW/m^2 at $9D$ downstream, while in the elbow cases, no such trend was observed. For a volume flow rate of 20 L/min, the wall heat flux reached a plateau of ~15 MW/m^2 at $4D$ and ~18 MW/m^2 at $9D$ downstream in the straight piping.

Contrarily, the downstream boiling curves of the elbow outlet revealed a decrease in the slopes as the heat flux increased, indicating an enhancement in the heat transfer performance in the elbow piping. However, no distinct cooling limit was observed.

4. Conclusion

In this study, visualization and heat transfer experiment using triple elbow piping were conducted to evaluate the applicability of the cooling system for a fusion divertor. The following findings were obtained:

(1) The multi-elbow generated swirling flow has a circumferential velocity of about up to 50% of the mean axial velocity in the fastest part. The swirling flow decayed as it moved downstream.

(2) In the high heat flux region of >10 MW/m^2, the swirling flow generated by the elbows led to a reduction in wall temperature. However, in the downstream region where the swirl flow was damped, the effect of the wall temperature reduction became smaller.

(3) In the case of straight piping, the wall heat flux seemed to reach a plateau. On the contrary, no obvious cooling limit was observed downstream of the elbow outlet. This suggests that the heat transfer performance is enhanced in the elbow piping.

Acknowledgment

This work was carried out with the support and under the auspices of the NIFS collaborative research program.

[1] K. Sato *et al.*, Development of ITER Divertor Plate with Annular Swirl Tube and Tungsten Rods, J. Plasma Fusion Res. SERIES **5**, 556 (2002).

[2] S. Kodate *et al.*, Feasibility Study of Application of a Self-formed Flow Field downstream of Elbows to Divertor Cooling, 21st International Conference on Nuclear Engineering (2013).

[3] S. Kodate *et al.*, Flow Visualization Experiment of a Swirling Flow Formed downstream of a Piping with Successive Three Elbow to be applied to Divertor Cooling, 22st International Conference on Nuclear Engineering (2014).

[4] S. Kodate *et al.*, Fundamental Study Application of Swirling Flow generated downstream of a Multi-elbow Layout to Divertor Cooling, The 20th National Symposium on Power and Energy System (SPES2015 in Japan)

[5] Y. Hamaji *et al.*, ACT2: High Heat Flux Test Facility Using Electron Beam for Fusion Application, Plasma Fusion Res. **11**, 2405089 (2016).

[6] W.M. Rohsenow, A method of correlation heat transfer data for surface boiling of liquids, Trans. ASME **74**, 969 (1952).

[7] A. Clark and W.M. Rohsenow, Trans. ASME **76**, 553 (1954).